








Gabriel K. Obiyenwa<sup>1</sup> , Banjo Semire<sup>1,2\*</sup> , Abel K. Oyebamiji<sup>3</sup> , Ibrahim O. Abdulsalami<sup>4</sup> , Dayo F. Latona<sup>5</sup> , Moriam D. Adeoye<sup>6</sup> , Olusegun A. Odunola<sup>2,7</sup> 

<sup>1</sup>Department of Chemistry, Federal University, Lokoja, Kogi State, Nigeria;

<sup>2</sup>Computational Chemistry Laboratory, Department of Pure and Applied Chemistry, Ladoke Akintola University of Technology, Ogbomosho, Nigeria;

<sup>3</sup>Industrial Chemistry Programme, Bowen University, Iwo, Osun State, Nigeria;

<sup>4</sup>Department of Chemistry, Nigerian Army University, Biu, Borno State, Nigeria;

<sup>5</sup>Department of Pure and Applied Chemistry, Osun State University, Osogbo, Nigeria;

<sup>6</sup>Department of Chemistry, Fountain University, Osogbo, Osun State, Nigeria;

<sup>7</sup>Department of Chemistry, Faculty of Natural and Applied sciences, Hallmark University, Ijebu-Itele, Ogun state, Nigeria

(\*Corresponding author's e-mail: [bsemire@jautech.edu.ng](mailto:bsemire@jautech.edu.ng))

## TD-DFT and DFT Investigation on Electrons Transporting Efficiency of 2-Cyano-2-Pyran-4-Ylidene-Acetic Acid and 2-Cyanoprop-2-Enoic Acid as Acceptors for Thiophene-Based $\pi$ -Linkers Dye-Sensitized Solar Cells

Great attention is being shifted to Dye-sensitized solar cells because of their structural and electronic tunability, high performance, and low cost compared to conservative photovoltaic devices. In this work, B3LYP/6-31G\*\* level of theory was used to study the molecular architecture of the donor- $\pi$ -acceptor (D- $\pi$ -A) type. This architecture contains a series of dyes with the 2-cyano-2-pyran-4-ylidene-acetic acid (PLTP-dye) and 2-cyanoprop-2-enoic acid (CLTP-dye) units as acceptors; donor groups and thiophene-based  $\pi$ -linkers. The molecular and electronic properties, light harvesting efficiency, open circuit voltage ( $V_{oc}$ ), injection force ( $\Delta G^{inject}$ ), regeneration force ( $\Delta G^{regen}$ ) and excitation state lifetime ( $\tau_{est}$ ) were calculated. CLTP-dyes showed lower band gap, chemical hardness ( $\eta$ ), chemical potential ( $\mu$ ), higher electrophilicity ( $\omega$ ) and electron denoting power ( $\omega^-$ ) than the corresponding PLTP-dyes. The  $\omega^-$  demonstrated that PLTP-1, PLTP-2 and PLTP-3, CLTP-1, CLTP-2 and CLTP-3 should readily push electrons to the  $\pi$ -linker, which can lead to high intra-molecular charge transfer and photocurrent for the dyes. The  $V_{oc}$  and  $\Delta G^{inject}$  parameters favoured the CLTP-dyes over corresponding PLTP-dyes, and also dyes with the N,N-diphenylaniline donor have higher  $V_{oc}$ ,  $\Delta G^{inject}$  values and longer wavelengths ( $\lambda_{max}$ ) than the dyes with carbazole unit (N,N-diphenylaniline dyes > Carbazole dyes) in accordance with the calculated  $\omega^-$ , although all the dyes have good regeneration and injection abilities.

**Keywords:** frontier orbitals, photoelectric properties, reactivity indices, TD-DFT, DFT, B3LYP, D- $\pi$ -A type, dye-sensitized solar cells (DSSC).

### Introduction

Increasing energy consumptions coupled with the global warming effect determined by energy supply from fossil resources has caused significant interest in renewable energy research. The energy released by the Sun to the Earth per hour exceeds the current world energy consumption per year; therefore, there is a daily growing in the development and use of solar renewable energy [1]. Consequently, efficient solar energy conversion devices or methods are required to provide a promising technology that can counterbalance the ever-growing energy demand needed for fast industrial development [2, 3]. However, solar photovoltaic cell has been considered to be one of the foremost prospective to cover a higher percentage of the future energy needs among other available renewable energy sources. In order to exploit this great benefit, a safe, cost-effective, efficient and ecofriendly method of harvesting solar energy are needed, and dye-sensitized solar cells (DSSCs) which belong to the third-generation solar cell technologies have the potential to meet these requirements. DSSCs invented by O'Regan and Grätzel in 1991, gave the broad view of using molecular components-based devices for the construction of a large-scale solar facility for electricity production, and thus put the solid-state technology to challenge by operating photovoltaic devices at molecular or nanoscale levels [4]. Although research is still ongoing, as well as pre-industrial technology in DSSCs is still low com-

pared to the performance of silicon devices; the efficiency is still below 13 % for DSSC [5]. Over the years, the applications of DSSCs have been intensively studied as a result of its potentially low cost of production, despite its current low efficiency and stability [6]. Designing of dye-sensitizers for DSSC have inform of donor (D)- $\pi$  spacer-acceptor (A) to ensure intra-molecular charge transfer, usually from donor unit through  $\pi$  spacer to the acceptor unit [7, 8]. In an attempt to improve the dye-sensitizers importance, different types of dyes combinations have been developed, such as D- $\pi$ -D- $\pi$ -A, (D- $\pi$ -A)<sub>2</sub>, D-A- $\pi$ -A, D-D- $\pi$ -A, D- $\pi$ -A-A and A- $\pi$ -D- $\pi$ -A [9–13].

Organic dyes with triphenylamine-based donor groups and the cyanoacrylic dyes as an acceptor/anchoring group are known for their outstanding properties, which have attracted much attention in DSSC technology [14–16]. Triphenyl moiety containing organic dyes possess unique characteristics such as the tunable frontier orbital energies, low dye aggregation, high molar absorption coefficients and non-planarity. These notable properties have made the triphenylamine (TPA) based sensitizers highly suitable for the DSSCs application [17]. However, these properties have led to a low recombination and back-reaction rate in the solar energy conversion process. Though,  $\pi$ -conjugated systems of the sensitizing dyes can be easily modified to obtain desired absorption wavelengths by adjusting the band gap of dyes [14, 15].

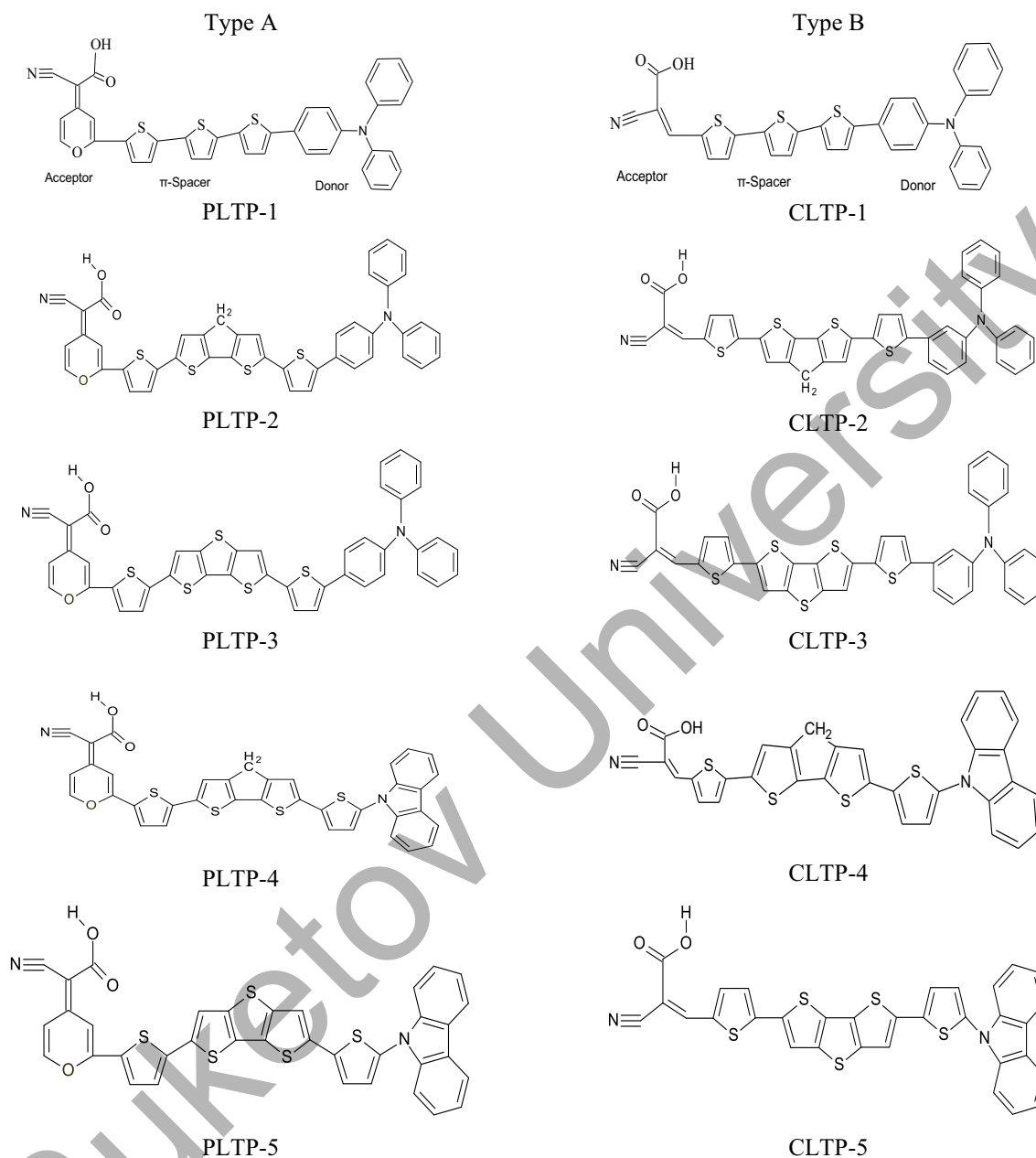
The cyanoprop-2-enoic acid has been a popular acceptor moiety for anchoring dye-sensitizers to TiO<sub>2</sub> surface in dye sensitized solar cells [16, 5]. However, other acceptor moieties used such dyes like the rhodamine-3-acetic acid in which the photovoltaic results were compared with those of the cyanoprop-2-enoic acid acceptor. The results revealed that dye with the rhodamine-3-acetic acid as an acceptor unit had the shorter wavelength, lower molar extinction coefficients and lower light capturing ability due to the weaker intra-molecular charge transfer ability [18]. Also, in some of our recent works, a series of dyes with the cyano-2-pyran-4-ylidene-acetic acid as acceptor were computationally modeled and studied. The results predicted very good optical properties, light harvesting efficiency and high circuit voltage, which were improved by the presence of fluorine atoms in the cyano-2-pyran-4-ylidene-acetic acid [19, 20]. Besides, several dyes of pyran derivatives have been investigated for absorption, light harvesting, intra-molecular charge transfer, regeneration and recombination properties using computational methods [21]; the results predict their applications as organic light emitting diode (OLED), bulk-heterojunction solar cells, and sensors [21–25].

Density functional theory (DFT) methods continue to play a leading role in the design and research of the electronic structure, photocurrent and electron transport properties of dye-sensitizers for photovoltaic applications such as DSSCs development [26–31]. Therefore, in this present study, density functional theory was used to explore the electron transporting efficiency of the 2-cyano-2-pyran-4-ylidene-acetic acid (type A dyes) and the 2-cyanoprop-2-enoic acid (type B dyes) as the acceptor anchoring units for thiophene-based  $\pi$ -linkers for dye-sensitized solar cells as shown in Table 1. The effects of these acceptor units on intra-molecular charge transfer, electrons regenerating, electrons injecting and light harvesting efficiency of the dye sensitizers were studied. The roles of thiophene derivatives (bisthieno[3,2-b,3-b]thiophene, 4H-cyclopenta[1,2-b,5,4-b]bisthiophene and terthiophene) as the  $\pi$ -linkers have thoroughly investigated and discussed.

#### *Computational Details*

The accuracy of DFT calculations depends on the selected functional and basis sets. It has been established that the polarized split-valence 6-31G(d, p) basis sets is sufficiently accurate for calculating the electronic excitation properties of organic dyes without extension of the basis sets [32, 33]; thus the designed D- $\pi$ -A dyes were optimized using DFT of the three-parameter density functional, with Becke's gradient exchange correction [34] and the Lee, Yang, Parr correlation functional (i.e. B3LYP) [35] accounting the 6-31G(d, p) basis set. Frequency calculations were performed on the optimized structures of the dyes at the same levels of theory to reveal the stationary points as local minima, and none of the optimized structures of the dyes exhibited imaginary frequencies. The frontier orbital energies, reactivity indices, natural density analysis, photo-electronics properties, intra-molecular charge transfer properties, and injection and regeneration driving forces were calculated. All calculations were carried out using Spartan 14 software from Wavefunction Inc. (Spartan, 2014) [36], implemented on an Intel® Core TM i7-4520M CPU, 2.50 GHz computer.

**Schematic structure of the studied molecules: Type A is the 2-cyano-2-pyran-4-ylidene-acetic acid and Type B is the 2-cyanoprop-2-enoic acid as acceptor anchor, respectively**



## Results and Discussion

### Frontier Molecular Orbital energies and reactivity indices

The frontier orbital energies, such as the HOMO and LUMO energies of dye sensitizers, are vital for modification the redox potential of the electrolyte and conduction-band edge of the semiconductor in DSSCs to achieve high harvesting and desired capability of the dye [37]. Designing low-molecular weight D- $\pi$ -A dye sensitizers require fine tuning the properties of frontier orbitals because they are qualitative characteristics of organic dyes excitation properties [38, 26, 27, 29]. The frontier orbitals contour overlay is displayed in Figure 1 shows that the HOMOs overlaid are localized on the donor subunit extended over  $\pi$ -linker, and also the LUMOs overlaid are mainly on acceptor subunit with extension over  $\pi$ -linker. This means that there is a good interaction between the donor and acceptor groups through  $\pi$ -linker, which could facilitate intramolecular charge transfer from donor to acceptor unit [39].

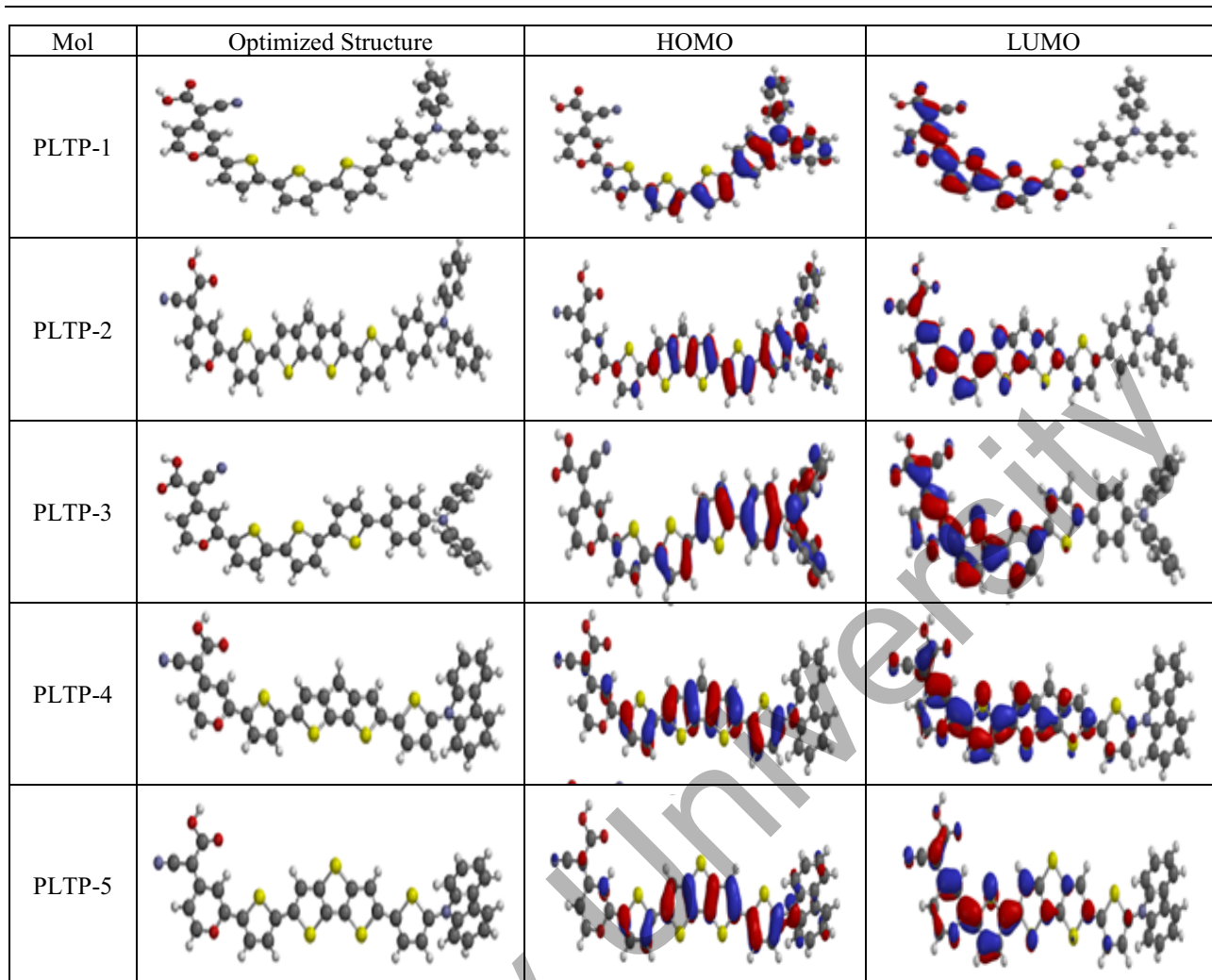
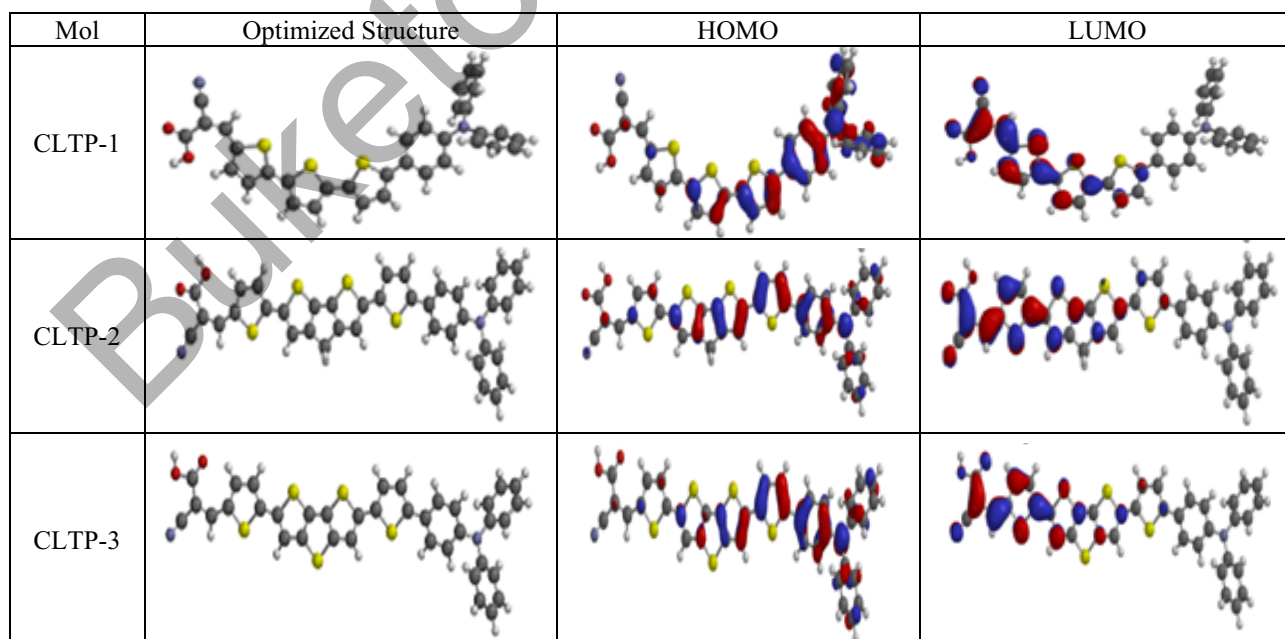


Figure 1a. The Contour Plots of the frontier orbitals of PLTPs dyes



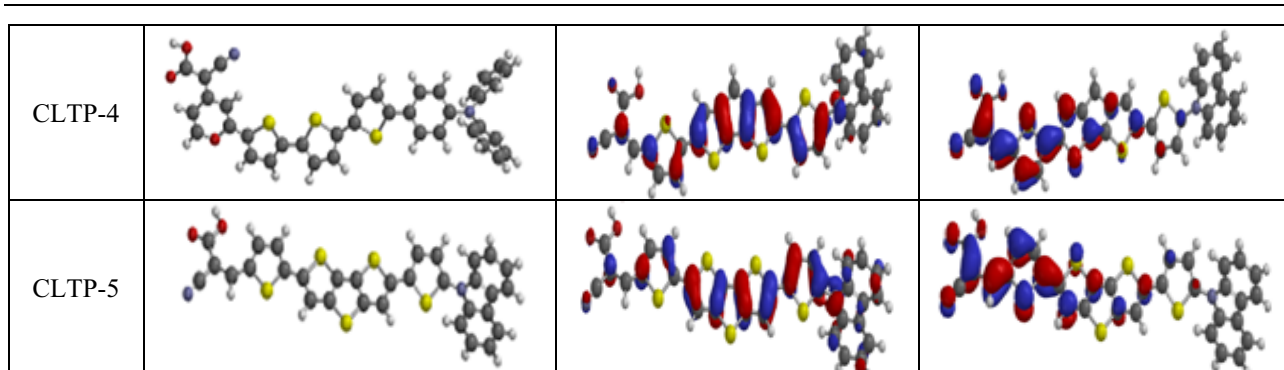
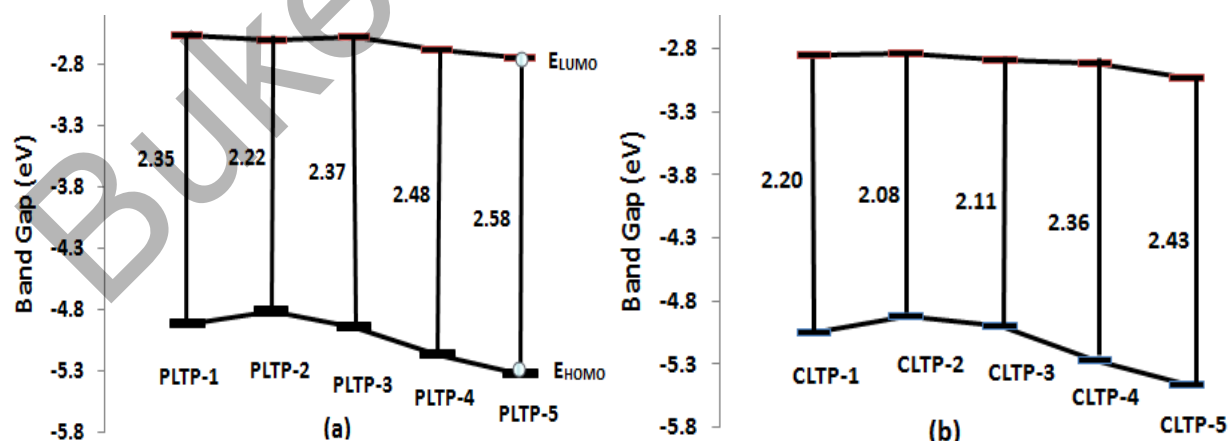


Figure 1b. The Contour Plots of frontier orbitals of CLTPs dyes

The electron accepting efficiency of the dye acceptors (types A and B) were examined by considering dyes with similar donors and  $\pi$ -conjugated linkers such as CLTP-1 and PLTP-1, CLTP-2 and PLTP-2, CLTP-3 and PLTP-3, CLTP-4 and PLTP-4, CLTP-5 and PLTP-5 (Lu et al., 2011 [40]). The HOMO, LUMO, and HOMO–LUMO energy gap ( $E_g$ ) for the dyes were calculated as  $-4.92$ ,  $-2.57$  and  $2.35$  eV for PLTP-1;  $-5.04$ ,  $-2.84$  and  $2.20$  eV for CLTP-1, respectively. The CLTP-1 dye (Type B) with the 2-cyanoprop-2-enoic acid as acceptor unit showed a decrease in both the HOMO and LUMO energies by  $0.12$  and  $0.27$  eV, respectively, which resulted into lowering of  $E_g$  by  $0.15$  eV for CLTP-1 compare to PLTP-1. The calculated HOMO, LUMO, and  $E_g$  values for PLTP-2 were  $-4.82$ ,  $-2.60$ ,  $2.22$  eV; and  $-4.91$ ,  $-2.83$  and  $2.08$  for CLTP-2, which also showed a reduction of the HOMO/LUMO by  $0.09/0.23$  eV resulting in a decrease of  $E_g$  by  $0.14$  eV for CLTP-2 over PLTP-2. Moreover, the HOMO, LUMO, and  $E_g$  for PLTP-3 were  $-4.94$ ,  $-2.67$ , and  $2.27$  eV; and  $-4.99$ ,  $-2.88$  and  $2.11$  eV for CLTP-3; this led to a relative decrease in the HOMO/LUMO by  $0.05/0.21$  eV resulting in a reduction of  $E_g$  by  $0.16$  eV for CLTP-3 compare to PLTP-3 (Fig. 2).

Similarly, the HOMO, LUMO and  $E_g$  for CLTP-4 was lowered by  $0.12$  eV as compare to PLTP-4 due to a decrease in the HOMO/LUMO by  $0.01/0.22$  eV. This observation revealed that both the HOMO and LUMO of type B dye's orbitals are delocalized leading relative ease of  $\pi$ -electrons flow, thus lowering of  $E_g$  in CLTP dyes. The  $E_g$  values of the studied dyes can be ordered as PLTP-2 < PLTP-1 < PLTP-3 < PLTP-4 < < PLTP-5 for type A, and CLTP-2 < CLTP-3 < CLTP-1 < CLTP-4 < CLTP-5 for type B (Fig. 2). Generally, type B presented lower band gap than the corresponding type A; however, all the dyes are good photosensitized prospects, since their HOMO energy levels are lower than the redox potential of the  $I^-/I_3^-$  electrolyte ( $-4.8$  eV) and LUMO energy levels are higher than the conduction band (CB) of the  $TiO_2$  semiconductor ( $-4.0$  eV) which ensures the injection of the electron from the dye to  $TiO_2$  as well as dye renaissance [40; 41].



*a* — 2-cyano-2-pyran-4-ylidene-acetic acid; *b* — 2-cyanoprop-2-enoic acid as acceptor anchor, respectively

Figure 2. Energy band gap for the studied D- $\pi$ -A dye sensitizers

Furthermore, the effect of  $\pi$ -linkers on the intramolecular charge transfer was investigated in the two-dye series; PLTP-1, PLTP-2 and PLTP-3 for type A, and CLTP-1, CLTP-2 and CLTP-3 for type B. The frontier energies (HOMO, LUMO and  $E_g$ ) for PLTP-1, PLTP-2 and PLTP-3 were (−4.92, −2.57 and 2.35 eV), (−4.82, −2.60, 2.22 eV) and (−4.95, −2.58 and 2.37 eV), respectively. Therefore, the use of 4H-cyclopenta[1,2-b,5,4-b]bisthiophene as  $\pi$ -linker in PLTP-2 increases/decreases the HOMO/LUMO energy by 0.10/0.03 eV compare to PLTP-1 with terthiophene as  $\pi$ -linker, thereby causing delocalization of the LUMO orbital leading to reduction in the  $E_g$  by 0.13 eV. However, with bisthieno[3,2-b,3-b]thiophene as  $\pi$ -linker in PLTP-3, the HOMO/LUMO was slightly decreased by 0.04/0.01 eV, thus PLTP-3 only increased in  $E_g$  by 0.02 eV. Also, similarly, the frontier orbital energies (HOMO, LUMO and  $E_g$ ) for CLTP-1, CLTP-2 and CLTP-3 were (−5.04, −2.84, 2.20 eV), (−4.91, −2.83, 2.08 eV) and (−4.99, −2.88 and 2.11 eV), respectively. The electronic properties revealed that the HOMO/LUMO energies of CLTP-2 (with 4H-cyclopenta[1,2-b,5,4-b]bisthiophene as  $\pi$ -linker) increases by 0.13/0.01 eV, leading to lowering of  $E_g$  by 0.12 eV compare to CLTP-1. At the same time, with bisthieno[3,2-b,3-b]thiophene as  $\pi$ -linker in CLTP-3, the HOMO/LUMO energies increases/decreases by 0.05/0.04 eV, which leads to reduction in  $E_g$  by 0.09 eV compare to CLTP-1 (Fig. 2). This suggests that dyes with 4H-cyclopenta[1,2-b,5,4-b]bisthiophene as linker could have superior photocurrent and charge transfer (CT) than dyes with terthiophene and bisthieno[3,2-b,3-b]thiophene as  $\pi$ -linkers (Semire et al., 2017 [48]), It can be argued that higher HOMO energy together with the lower LUMO energy favors excitation of electrons in D– $\pi$ –A organic dyes [21].

In addition, the efficiency of the donor subunits was also investigated by considering CLTP-2 and CLTP-4, PLTP-2 and PLTP-4 dyes. Comparing CLTP-2 and CLTP-4, the HOMO, LUMO energies, and  $E_g$  were −5.27, −2.91, 2.36 eV for CTP-4; and −4.91, −2.83 and 2.08 eV for CLTP-2. There is a stabilization of both the HOMO and LUMO orbitals by 0.36 and 0.08 eV, respectively leading to enhancement of  $E_g$  by 0.28 eV in CLTP-2 dyes compare to CLTP-4. Also, comparing PLTP-4 and PLTP-2, it can be noted that  $E_g$  enhanced by 0.26 eV as a result of stabilization of both the HOMO/LUMO by 0.35/0.09 eV. Therefore, N,N-diphenylaniline donor group donors/pushes more electrons readily towards  $\pi$ -linker than carbazole donor group, thus dyes bearing N,N-diphenylaniline donor group should have better intramolecular charge transfer and good photocurrent ability [20].

The natural bond orbital (NBO) analysis was performed on the optimized structure in the ground state in order to study the electron transfer mechanism as well as charge distribution of the studied D– $\pi$ –A dyes. The calculated NBOs at the B3LYP/6-31G (d, p) level are listed in Table 2. The positive charges on the N,N-diphenylaniline moiety reveals an efficacious electron-donor unit and the large negative NBO charges on 2-cyano-2-pyran-4-ylidene-acetic acid/2-cyanoprop-2-enoic acid are evidence that electrons are enthralled in the acceptor unit. The NBO analysis, N-diphenylaniline donor group shows that the cyano-substituent attached to the acceptor unit of the dyes increases/decreases the natural bond orbital charges on both the acceptor and donor units. The trapping of electrons in the acceptor unit denotes that the NBO charges in the dye sensitizers are subjugated by acceptor moieties [42].

The dyes electronegativity ( $\chi$ ), chemical hardness ( $\eta$ ), electrophilicity index ( $\omega$ ) and electron donating power ( $\omega^-$ ) were estimated from the ground state geometries of the optimized dyes at B3LYP/6-31G\*\* level of theory for an N-electron system with total energy E as described in equations 1–4 [42, 43].

$$\chi = -\mu = \left( \frac{\delta E}{\delta N} \right)_{v(r)} \cong \frac{IP + EA}{2} \quad (1)$$

$$\eta = \left( \frac{\delta^2 E}{\delta N^2} \right)_{v(r)} \cong \frac{IP - EA}{2} \quad (2)$$

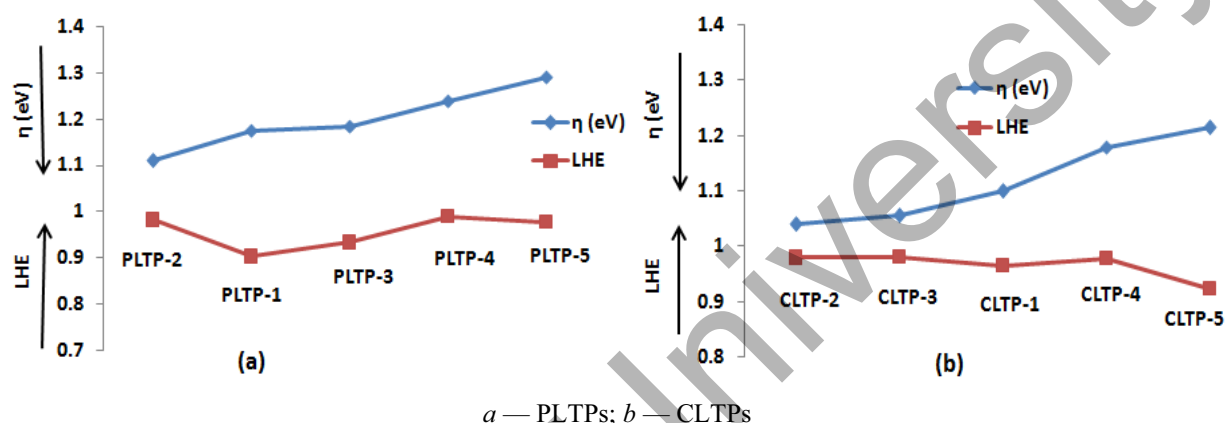
$$\omega = \frac{\mu^2}{2\eta} = \frac{(IP + EA)^2}{4(IP - EA)} \quad (3)$$

$$\omega^- = \frac{(3IP - EA)^2}{16(IP - EA)} \quad (4)$$

where IP (vertical ionization potential) and EA (vertical electron affinity) are approximated to  $-E_{HOMO}$  and  $-E_{LUMO}$ , respectively [45].

Global Molecular Descriptors and Light Harvesting Efficiency (LHE)

MOL	q <sub>Donor</sub>	$\pi$ -linker	q <sub>Acceptor</sub>	$\Delta q(D-A)$	$\mu$ (eV)	$\eta$ (eV)	$\omega$ (eV)	$\omega^-$ (eV)
PLTP-1	0.126	-0.006	-0.120	0.246	-3.745	1.175	5.968	3.952
PLTP-2	0.142	-0.008	-0.138	0.280	-3.710	1.110	6.200	3.960
PLTP-3	0.141	-0.002	-0.140	0.281	-3.765	1.185	5.981	3.970
PLTP-4	0.152	0.019	-0.153	0.305	-3.930	1.240	6.227	4.142
PLTP-5	0.130	-0.004	-0.133	0.263	-4.040	1.290	6.325	4.247
CLTP-1	0.127	0.001	-0.125	0.252	-3.940	1.100	7.055	4.284
CLTP-2	0.033	-0.036	-0.172	0.205	-3.870	1.040	7.200	4.255
CLTP-3	0.135	-0.024	-0.164	0.299	-3.935	1.055	7.338	4.330
CLTP-4	0.143	-0.013	-0.132	0.275	-4.090	1.180	7.088	4.407
CLTP-5	0.142	-0.009	-0.136	0.278	-4.245	1.215	7.415	4.584

Figure 3: Relationship between light harvesting efficiency (LHE) and chemical hardness ( $\eta$ ):

The thermodynamic stability of dye-sensitizers, a crucial parameter was adjudged by reactivity indices. Chemical hardness ( $\eta$ ) is a parameter associated with molecular resistance to charge transfer with the surrounding [19]. According to [48] (Semire et al., 2017) it has a very close relation to intra-molecular charge transfer is favoured by low  $\eta$  for good dye-sensitizers. The  $\eta$  shows that type B (CLTP dyes) have lower chemical hardness compare to type A (PLTP dyes). The relationship between  $\eta$  and LHE has been described as a graph funnel-like shape [46]. Thus, as shown in Figure 3, low  $\eta$  and high LHE enhance good photocurrent in DSSCs [46] leading to a better short circuit current density ( $J_{sc}$ ). Chemical potential ( $\mu$ ) is a parameter relating to charge transfer ability of a dye in its ground state, this is enhanced by high negative value of  $\mu$  (Table 2). The electrophilicity ( $\omega$ ) describes the stabilization energy of a dye when an electronic charge is added to the dye from the surrounding, therefore, a high  $\omega$  is desirable for good energy stabilization. All the dyes exhibit very good stabilization energy; however, type B (CLTP dyes) is more stabilized than type A (PLTP dyes). The electron denoting power ( $\omega^-$ ) is related to the ability of the dye to donate/push electrons through the linker/spacer to the acceptor unit of a dye. So, low value of  $\omega^-$  corresponds to a better ability of donating/pushing electron density towards acceptor [46, 47]. Therefore, PLTP-1, PLTP-2 and PLTP-3 of type A and CLTP-1, CLTP-2 and CLTP-3 of type B will readily push electrons to the  $\pi$ -linker, leading to high intramolecular charge transfer and thus high photocurrent in DSSCs [48], suggesting higher electron-donating ability of dyes with N, N-diphenylaniline donor unit.

#### Theoretical view of the dye's efficiency

The light harvesting efficiency (LHE) is expected to be as high as possible for the dye sensitizers to have good performance in DSSC, also to enhance the photocurrent if the excited processes have a CT character. Therefore, the LHEs of the studied dyes are calculated as [49]:

$$LHE = 1 - 10^{-A} = 1 - 10^{-f} \quad (5)$$

where  $f$  is the oscillator strength of the excited state associated to the  $\lambda_{max}$  and  $A$  is the absorption coefficient.

The LHE values reveal that PLTP-2, PLTP-4 and PLTP-5 for type A dyes, and CLTP-3, CLTP-2 and CLTP-4 for type B dyes are favoured for higher photocurrent (Table 3). Also, another key parameter of molecular global descriptors of solar cells is the open circuit voltage ( $V_{oc}$ ) [35]. It is well known that the larger value  $V_{oc}$  corresponds to the better performance of solar cells [50].  $V_{oc}$  is interrelated by the difference between the LUMO energy of the dye-sensitizer and the conduction band (the LUMO) of the electron acceptor ( $TiO_2$ ;  $-4.0$  eV), taking into account the energy lost during the photo-charge generation [51; 52]. The  $V_{oc}$  of the studied solar cell can be estimated by Equation (6) [44]:

$$V_{oc} = E_{LUMO} - E_{CB}^{TiO_2} \quad (6)$$

The calculated  $V_{oc}$  values were 1.43, 1.40, 1.42, 1.31 and 1.25 for PLTP-1 to PLTP-5; and 1.16, 1.17, 1.12, 1.09 and 0.97 for CLTP-1 to CLTP-5, respectively (Table 3). This shows that  $V_{oc}$  values for type A dyes are higher than for the corresponding type B dyes; therefore, they are expected to present higher injection driving force and power conversion efficiency than type B. This also reveals that dyes with N,N-diphenylaniline donor unit have a higher  $V_{oc}$  value than dyes with carbazole unit (N,N-diphenylaniline dyes > Carbazole dyes) in line with calculated  $\omega^-$  (Table 2).

The electron injecting ability ( $\Delta G^{inject}$ ) of the dyes were estimated for the two dyes series of dye-sensitizers (i.e. PLTPs and CLTPs) from the oxidation potential of the excited dye ( $E_{ox}^{dye^*}$ ) and the redox potential of the dye- $TiO_2$  couples [47]:

$$\Delta G^{inject} = E_{ox}^{dye^*} - E_{CB}^{TiO_2} \quad (7)$$

However,  $E_{ox}^{dye^*}$  was calculated as the difference in the ground state oxidation potential of the dye and vertical electronic transition energy ( $\lambda_{max}^{ICT}$ ) [14].

$$E_{ox}^{dye^*} = E_{ox}^{dye} - \lambda_{max}^{ICT} \quad (8)$$

and the driving force of the dye regeneration known as regeneration efficiency ( $\Delta G^{regen}$ ) was estimated using Equation 9 [15].

$$\Delta G^{regen} = E_{ox}^{dye} - E_{redox}^{electrolyte} \quad (9)$$

where 4.70 eV was taken as the value of  $E_{redox}^{electrolyte}$  [44].

The negative values of injection driving force ( $\Delta G^{inject}$ ) show the ability of the dyes to inject electrons readily into  $TiO_2$  surface as shown in Table 3. The  $\Delta G^{inject}$  values show that PLTP-1, PLTP-3 for type A dyes, and CLTP-1, CLTP-2 and CLTP-3 for type B dyes are considered the best dyes, for they presented higher  $\Delta G^{inject}$  values than PLTP-2, PLTP-4, PLTP-5, CLTP-4 and CLTP-5 (Table 3), signifying easy electrons injection into  $TiO_2$ . The positive values of dye regeneration drive force ( $\Delta G^{regen}$ ) suggest fast electrons transfer and thus ability to regenerate. However, it is necessary for  $\Delta G^{regen}$  be as low as possible, making PLTP-2, CLTP-2, PLTP-1, PLTP-3 and CLTP-3 to be the candidate dyes for greater power conversion efficiency [53]. Another parameter to adjudge the suitability of a dye-sensitizer is the excitation state lifetime ( $\tau_{esl}$ ), a critical parameter for the charge-transport characteristics of a dye. It was predicted using Equation 10 [53; 54]:

$$\tau_{esl} = \frac{1.499}{fE^2} \quad (10)$$

where E is the excitation energy of different electronic states in  $cm^{-1}$ , and f is the oscillator strength corresponding to the electronic state.

The  $\tau_{esl}$  values reveal that CLPT-4 (2.576 ns), CLTP-5 (2.479 ns), PLTP-2 (2.998 ns) and PLTP-1 (1.647 ns) could be more stable in the cationic state, leading to long-lived excited state, higher charge transfer efficiency and improved efficiency of the dye-sensitizers than dyes with lower  $\tau_{esl}$  [54].

Table 3

**Calculated driving force of electron rejection and dye regeneration, LHE, Voc and excited state lifetimes ( $\tau$ )**

MOL	$\lambda_{max}^{ICT}$	f	$E_{ox}^{dye^*}$	$\Delta G_{inj}$	$\Delta G_{reg}$	Voc	LHE	$\tau$ (ns)
PLTP-1	2.714	1.0117	2.206	-1.794	0.22	1.43	0.9026	1.932
PLTP-2	2.041	1.7299	2.779	-1.221	0.12	1.40	0.9813	2.998
PLTP-3	2.731	1.1766	2.219	-1.781	0.25	1.42	0.9334	1.647
PLTP-4	2.319	1.9851	2.851	-1.149	0.47	1.31	0.9896	1.349

MOL	$\lambda_{max}^{ICT}$	$f$	$E_{ox}^{dye*}$	$\Delta G_{inj}$	$\Delta G_{reg}$	Voc	LHE	$\tau(ns)$
PLTP-5	2.368	1.6574	2.962	-1.038	0.63	1.25	0.9779	1.550
CLTP-1	2.701	1.4629	2.339	-1.661	0.34	1.16	0.9655	1.350
CLTP-2	2.465	1.6913	2.445	-1.555	0.21	1.17	0.9796	1.401
CLTP-3	2.502	1.7410	2.488	-1.512	0.29	1.12	0.9818	1.322
CLTP-4	2.279	1.0761	2.991	-1.010	0.57	1.09	0.9776	2.576
CLTP-5	2.284	1.1136	3.176	-0.824	0.76	0.97	0.9230	2.479

### Photo-electronic Properties

The Beer–Lambert law states that absorbance at higher level denotes higher dye application. The study of the correlation between the DSSC photocurrent and the number of dye molecules has become trendy. In view of this, larger photocurrent can be attributed to increased adsorbed dye, ensuing in the increased harvesting of incident light [55–60]. Atomic information with reference to the electronic transitions can be obtained by investigating the molecular orbitals associated with each electronic transition, as calculated at TD-DFT/6-31G(d, p) level of theory (Tables 4). Absorptions in the visible and near-ultraviolet (UV) regions of the spectrum are the most important for photo to current conversion, so only the singlet  $\rightarrow$  singlet transitions of the absorption bands with the wavelength longer than 300 nm are listed in the Table 4. The maximum absorbent wavelengths ( $\lambda_{max}$ ) with probability of electron transition (oscillating strength,  $f$ ) for the type A; PLTP-1, PLTP-2, PLTP-3, PLTP-4 and PLTP-5 were 579.02 (0.7881), 600.75 (1.7299), 570.36 (1.009), 528.81 (1.951) and 517.87 nm (1.6574), respectively, all arising from H $\rightarrow$ L orbital transitions. It is interesting to note that two major electronic transitions with highest  $f$  are arisen from the H $\rightarrow$ L and H-1 $\rightarrow$ L orbitals' transitions (Table 4a). The maximum absorption transitions for type A dyes decreases in the following order: PLTP-2 > PLTP-1 > PLTP-3 > PLTP-4 > PLTP-5. Furthermore, the  $\lambda_{max}$  with oscillating strength,  $f$  for CLTP-1, CLTP-2, CLTP-3, CLTP-4 and CLTP-5 were 609.58 (0.7484), 626.50 (1.4056), 631.16 (1.0761), 537.94 (1.6503) and 536.83 (1.1136) nm, respectively, all arising from H $\rightarrow$ L orbitals' transitions as observed for type A. Similarly, the two major electronic transitions with highest  $f$  are arisen from the H $\rightarrow$ L and H-1 $\rightarrow$ L orbitals' transitions (Table 4b), and the maximum absorption transitions for type B dyes decreases as follows: CLTP-3 > CLTP-2 > CLTP-1 > CLTP-4 > CLTP-5.

To compare the effect of  $\pi$ -linkers of electronic transitions as it relates to intramolecular charge transfer, PLTP-2 (CLTP-2) and PLTP-3 (CLTP-3) were considered. The 4H-cyclopenta[1,2-b,5,4-b]bisthiophene  $\pi$ -linker was changed in PLTP-2 (CLTP-2) to bithioeno[3,2-b,3-b]thiophene as presented in PLTP-3 (CLTP-3). There was a shift in  $\lambda_{max}$  to shorter wavelength (blue-shift) by 30 and 4 nm, respectively; which may be due to easier delocalization of  $\pi$ -electrons for 4H-cyclopenta[1,2-b,5,4-b]bisthiophene  $\pi$ -linker than bithioeno[3,2-b,3-b]thiophene leading to extension of  $\pi$ -conjugation [48]. To adjudge the effect of donor groups on intracrossing charge transfer as it reflected in electronic transitions, PLTP-2 (CLTP-2) and PLTP-4 (CLTP-4) were considered. Replacement of N,N-diphenylamine in PLTP-2 (CLTP-2) with carbazole in PLTP-4 (CLTP-4) shifted the  $\lambda_{max}$  to shorter wavelength (blue shift) of about 72 (90) nm, indicating that N,N-diphenylaniline pushes electrons more readily towards the linker than carbazole donor which is in line with the frontier orbital interactions and Eg energy earlier observed. Generally, **type B** dyes present lower energy energies and longer  $\lambda_{max}$  than the corresponding **type A** dyes, which may be linked to effective delocalization of  $\pi$ -electrons for 2-cyanoprop-2-enoic acid acceptor bearing dyes, and so enhance longer wavelength.

Table 4 a

### Absorption peaks, oscillation strength and molecular orbital's (MOs) involved in transitions calculated for PLTPs using B3LYP/6-31G (d, p)

$\lambda$ , nm	OS	MOs involved in transition
PLTP-1		
350.57	0.2312	H-1 $\rightarrow$ L+1 (63 %)
367.83	0.2710	H $\rightarrow$ L +2 (81 %)
394.99	0.1113	H-2 $\rightarrow$ L (63 %), H-1 $\rightarrow$ L+1 (20 %),
428.85	0.2152	H $\rightarrow$ L+1 (81 %)
451.85	1.0117	H-1 $\rightarrow$ L (86 %)
579.02	0.7861	H $\rightarrow$ L (96 %)

Continuation of Table 4a

$\lambda$ , nm	OS	MOs involved in transition
PLTP-2		
378.42	0.0970	H-1 $\rightarrow$ L+1 (54 %), H-2 $\rightarrow$ L (20 %)
392.12	0.0840	H $\rightarrow$ L+2 (66 %), H-3 $\rightarrow$ L (22 %)
409.36	0.0486	H-2 $\rightarrow$ L (49 %), H-1 $\rightarrow$ L+1 (35 %).
457.61	0.4318	H $\rightarrow$ L+1 (81 %)
486.49	1.2276	H-1 $\rightarrow$ L (89 %)
600.75	1.7299	H $\rightarrow$ L (97 %)
PLTP-3		
350.13	0.2415	H-1 $\rightarrow$ L+1 (66 %)
367.00	0.1481	H $\rightarrow$ L+2 (83 %)
394.57	0.0732	H-2 $\rightarrow$ L (64 %), H-1 $\rightarrow$ L+1 (18 %).
427.09	0.1730	H $\rightarrow$ L+1 (81 %)
449.08	1.1766	H-1 $\rightarrow$ L (88 %)
570.36	1.0098	H $\rightarrow$ L (98 %)
PLTP-4		
369.57	0.0049	H $\rightarrow$ L+2 (65 %), H-4 $\rightarrow$ L (29 %)
388.72	0.2378	H-3 $\rightarrow$ L (42 %), H $\rightarrow$ L+1 (26 %), H-1 $\rightarrow$ L+1 (17 %).
428.53	0.3541	H $\rightarrow$ L+1 (58 %), H-3 $\rightarrow$ L (38 %).
450.32	0.3635	H-1 $\rightarrow$ L (94 %)
528.81	1.9851	H $\rightarrow$ L (94 %).
PLTP-5		
366.12	0.0335	H-4 $\rightarrow$ L (85 %)
389.08	0.2185	H-3 $\rightarrow$ L (36 %), H $\rightarrow$ L+1 (28 %), H-1 $\rightarrow$ L+1 (23 %)
419.26	0.2816	H $\rightarrow$ L+1 (53 %), H-3 $\rightarrow$ L (42 %)
444.03	0.5918	H-1 $\rightarrow$ L (95 %)
517.87	1.6574	H $\rightarrow$ L (96 %)

Table 4b

**Absorption peaks, oscillation strength and molecular orbital's (MOs) involved in transition calculated for CLTPs using B3LYP/6-31G (d, p)**

$\lambda$ , nm	OS	MOs involved in transition
CLTP-1		
326.99	0.0694	H $\rightarrow$ L+4 (40 %), H-4 $\rightarrow$ L (18 %), H $\rightarrow$ L+3 (16 %)
339.04	0.0680	H $\rightarrow$ L+2 (45 %), H $\rightarrow$ L+3 (36 %).
361.61	0.2603	H-1 $\rightarrow$ L+1 (55 %), H-2 $\rightarrow$ L (32 %)
412.25	0.2996	H $\rightarrow$ L+1 (77 %)
454.06	1.4629	H-1 $\rightarrow$ L (83 %)
609.58	0.7484	H $\rightarrow$ L (97 %)
CLTP-2		
356.84	0.0086	H $\rightarrow$ L+2 (50 %), H-3 $\rightarrow$ L (20 %), H-1 $\rightarrow$ L+1 (14 %)
357.91	0.0060	H-2 $\rightarrow$ L (40 %), H $\rightarrow$ L+2 (29 %)
395.70	0.1449	H-1 $\rightarrow$ L+1 (63 %), H-2 $\rightarrow$ L (22 %)
449.92	0.5089	H $\rightarrow$ L+1 (77 %), H-2 $\rightarrow$ L (18 %)
497.36	1.6913	H-1 $\rightarrow$ L (86 %)
627.50	1.4056	H $\rightarrow$ L (94 %)
CLTP-3		
353.83	0.0073	H-2 $\rightarrow$ L (31 %), H-1 $\rightarrow$ L+1 (22 %), H $\rightarrow$ L+2 (13 %)
384.95	0.0672	H-3 $\rightarrow$ L (69 %), H-1 $\rightarrow$ L+1 (26 %)
390.88	0.2129	H-2 $\rightarrow$ L (40 %), H-1 $\rightarrow$ L+1 (30 %), H-3 $\rightarrow$ L (19 %)
442.01	0.6049	H $\rightarrow$ L+1 (79 %)
490.18	1.7410	H-1 $\rightarrow$ L (88 %)
631.16	1.0761	H $\rightarrow$ L (97 %)

Continuation of Table 4 b

$\lambda$ , nm	OS	MOs involved in transition
CLTP-4		
367.84	0.0226	H-1 $\rightarrow$ L+1 (81 %).
415.32	0.4898	H $\rightarrow$ L+1 (69 %), H-3 $\rightarrow$ L (28 %)
461.19	0.9159	H-1 $\rightarrow$ L (86 %)
537.94	1.6503	H $\rightarrow$ L (86 %)
CLTP-5		
370.99	0.1496	H-1 $\rightarrow$ L+1 (74 %)
382.82	0.0147	H-4 $\rightarrow$ L (68 %), H-3 $\rightarrow$ L (27 %).
405.72	0.6982	H $\rightarrow$ L+1 (72 %), H-3 $\rightarrow$ L (21 %).
462.95	1.1122	H-1 $\rightarrow$ L (88 %)
536.83	1.1136	H $\rightarrow$ L (89 %)

### Conclusions

This paper reports a comprehensive computational investigations on the efficiency of the 2-cyano-2-pyran-4-ylidene-acetic acid and the 2-cyanoprop-2-enoic acid units as acceptor units connected through the thiophene-based  $\pi$ -linker dyes for the improvement of dye-sensitizers for DSSCs using the DFT(B3LYP/6-31G(d, p) method. The results revealed the following:

(1) Dyes with 4H-cyclopenta[1,2-b,5,4-b]bis-thiophene as a  $\pi$ -linker exhibit narrower band gap, and the longer absorption wavelength than others dyes in each dye series, indicating better intra-molecular charge transfer;

(2) Dyes with N,N-diphenylamine as a donor unit presents lower band gaps, better the open circuit current ( $V_{oc}$ ) and longer  $\lambda_{max}$  wavelength than dyes with the carbazole donor unit, indicating that N,N-diphenylaniline pushes electrons readily towards the  $\pi$ -linker than the carbazole donor; thus represents the better donor group;

(3) **Type B** dyes present lower band gaps and longer  $\lambda_{max}$  wavelength than the corresponding **type A** dyes, indicating effective delocalization of  $\pi$ -electrons in dyes with the 2-cyanoprop-2-enoic acid acceptor anchoring unit. This leads to better intra-molecular charge transfer, enhanced longer wavelength, higher  $V_{oc}$  value and injection force.

### References

- 1 Park, SH, Leclerc, M, Heeger AJ & Lee K (2006). High Efficiency Polymer Solar Cells with Internal Quantum Efficiency Approaching 100 %. *Proc SPIE*, 74160. <https://doi.org/10.1117/12.825836>
- 2 Kammen, D.M. (2006). The rise of renewable energy. *Sci Am.*, 295, 84–93. <https://doi.org/10.1038/scientificamerican0906-84>
- 3 Chiba, Y., Islam, A., Watanabe, Y., Komiya, R., Koide, N. & Han L (2006). Dye-Sensitized Solar Cells with Conversion Efficiency of 11.1 %. *Japanese J Appl Phys L* 638–L640. <https://doi.org/10.1143/JJAP.45.L638>
- 4 Regan, B.O. & Grätzel, M., (1991) A low-cost, high-efficiency solar cell based on dye-sensitized colloidal TiO<sub>2</sub> films. *Nature* 353, 737–740. <https://doi.org/10.1038/353737a0>
- 5 Yella, A, Lee, H.W., Tsao, H.N., Yi, C., Chandiran, A.K., Nazeeruddin, M.K., Diau, W., Yeh, C.Y., Zakeeruddin, S.M. & Grätzel, M. (2011). Porphyrin sensitized solar cells with cobalt(II/III)-based redox electrolyte exceed 12 percent efficiency. *Science* 334, 629–634. <https://doi.org/10.1126/science.1209688>
- 6 Hagfeldt, H., Boschloo, G., Sun, L., Kloo, L. & Pettersson, H. (2010). Dye-sensitized solar cells. *Chem Rev* 110, 6595–6663. <https://doi.org/10.1021/cr900356p>
- 7 Qian, X., Gao, H-H, Zhu, Y-Z, Pan, B. & Zheng, J-Y, (2015). Tetraindole-based saddle-shaped organic dyes for efficient dye-sensitized solar cells. *Dyes Pigments*. 121, 152–158. <https://doi.org/10.1016/j.dyepig.2015.05.015>
- 8 Jia, J., Chen, Y., Duan, L., Sun, Z., Liang, M. & Xue S. (2017). New D- $\pi$ -A dyes incorporating dithieno[3,2-b:2',3'-d]pyrrole (DTP)-based  $\pi$ -spacers for efficient dye-sensitized solar cells. *RSC Adv.* 7, 45807–45817. <https://doi.org/10.1039/C7RA08965A>
- 9 Semire, B., Odunola, O.A., Adejoro, I.A. (2012). Structural and electronic properties of 4H-Cyclopenta [2, 1-b, 3; 4-b'] di-thiophene S-oxide (BTO) With S, S= O, O, SiH<sub>2</sub> and BH<sub>2</sub> bridge: semi-empirical and DFT study. *J mol Model* 18, 2755–2760. <https://doi.org/10.1007/s00894-011-1291-1>

- 10 Zhang, C.R. Liu, L., Zhe, J.W., Jin, N.Z., Ma, Y., Yuan, L.H., Zhang, M.L., Wu, Y.Z., Liu, Z.J. & Chen, H.S. (2013). The Role of the Conjugate Bridge in Electronic Structures and Related Properties of Tetrahydroquinoline for Dye Sensitized Solar Cells. *Int J Mol Sci* 14, 5461–5481. <https://doi.org/10.3390/ijms14035461>
- 11 Ahn, H.J., Thogiti, S., Cho, J.M., Jang, B.Y. & Kim, J.H. (2015). Comparison of triphenylamine based single and double branched organic dyes in dye-sensitized solar cells. *Electronic Mater Lett* 11, 822–827. <https://doi.org/10.1007/s13391-015-4501-7>
- 12 Dindorkar, S.S. & Yadav, A., (2022). Insights from Density Functional Theory on the Feasibility of Modified Reactive Dyes as Dye Sensitizers in Dye-Sensitized Solar Cell Applications. *Solar* 2, 12–31. <https://doi.org/10.3390/solar2010002>
- 13 Roohi, H. & Mohtamadifar, N. (2022). The role of the donor group and electron-accepting substitutions inserted in  $\pi$ -linkers in tuning the optoelectronic properties of D- $\pi$ -A dye-sensitized solar cells: a DFT/TDDFT study. *RSC Adv.*, 121, 1557–11573. <https://doi.org/10.1039/D2RA00906D>
- 14 Hagberg, D., Marinado, T., Karlsson, K., Nonomura, K., Qin, P. & Boschloo, G. (2007). Tuning the HOMO and LUMO energy levels of organic chromophores for dye sensitized solar cells. *J Org Chem.* 72, 9550–9556. <https://doi.org/10.1021/jo701592x>
- 15 Marszalek, M., Nagane, S., Ichake, A., Baker, R., Paul, V. & Zakeeruddin, S. (2012). Tuning spectral properties of phenothiazine based donor- $\pi$ -acceptor dyes for efficient dye-sensitized solar cells. *J Mater Chem* 22, 889–894. <https://doi.org/10.1039/C1JM14024H>
- 16 Tan, L., Huang, J., Shen, Y., Xiao, L., Liu, J. & Kuang D. (2014). Highly efficient and stable organic sensitizers with duplex starburst triphenylamine and carbazole donors for liquid and quasi-solid-state dye-sensitized solar cells. *J Mater Chem A* 2, 8988–8994. <https://doi.org/10.1039/C4TA01351D>
- 17 Cheng, Y.J., Yang, S.H., Hsu, C.S. (2009). Synthesis of conjugated polymers for organic solar cell applications. *Chem Rev* 109, 5868–5923. <https://doi.org/10.1021/cr900182s>
- 18 Wang, X., Bolag, A., Yun, W., Zhang, X., Bao, T., Ning, J., Alata, H. & Ojayed, T. (2020). Synthesis, Characterization and Dye-Sensitized Solar Cell Application of a Novel Symmetric Diphenylpyran Dye with Dual Rhodamine-3-acetic Acid Anchors. *J Phys: Conf Series* 1549, 032072. <https://doi.org/10.1088/1742-6596/1549/3/032072>
- 19 Semire, B., Oyebamiji, A. & Odunola, O.A. (2016). Design of (2Z)-2-cyano-2-[2-[(E)-2-[5-[(E)-2-(4-dimethylamino-phenyl)vinyl]-2-thienyl]vinyl]pyran-4-ylidene]acetic acid derivatives as D- $\pi$ -A dye sensitizers in molecular photovoltaics: a density functional theory approach. *Res Chem Intermed* 42, 4605–4619. <https://doi.org/10.1007/s11164-015-2303-z>
- 20 Semire, B., Oyebamiji, A.K. & Odunola, O.A. (2020). Electronic properties' modulation of D-A-A via fluorination of 2-cyano-2-pyran-4-ylidene-acetic acid acceptor unit for efficient DSSCs: DFT-TDDFT approach. *Scientific African* 7, e00287. <https://doi.org/10.1016/j.sciaf.2020.e00287>
- 21 Joo, H.K. & Hoosung, L. (2002). Synthesis, electrochemistry, and electroluminescence of novel red-emitting poly(p-phenylenevinylene) derivative with 2-pyran-4-ylidenemalononitrile obtained by the heck reaction. *Chem Mater* 14, 2270–2275. <https://doi.org/10.1021/cm011553r>
- 22 Peng, Q., Lu, Z.Y., Huang, Y., Xie, M.G., Han, S.H., Peng, J.B. & Cao, Y. (2004). Synthesis and characterization of new red-emitting polyfluorene derivatives containing electron-deficient 2-pyran-4-ylidene- malononitrile moieties, *Macromolecules* 37, 260–266. <https://doi.org/10.1021/ma0355397>
- 23 Cui, Y., Jiancan, Y., Gao, J., Wang, Z. & Qian, G. (2009). Synthesis and luminescence behavior of inorganic-organic hybrid materials covalently bound with pyran-containing dyes. *Sci Technol* 52, 362–369. <https://doi.org/10.1007/s10971-009-2037-8>
- 24 Xue, J., Gu, X., Yang, Z., Xu, B. & Tian W. (2009). Efficient bulk hetero-junction solar cells based on a symmetrical D- $\pi$ -A- $\pi$ -D organic dye molecule. *J Phys Chem C* 113, 12911–12917. <https://doi.org/10.1021/jp902976w>
- 25 Son, Y.A., Gwon, S.Y., Lee, S.Y. & Kim, S.H. (2010). Synthesis and property of solvatochromic fluorophore based on D- $\pi$ -A molecular system: 2-[[3-Cyano-4-(N-ethyl-N-(2-hydroxyethyl)amino)styryl]-5,5-dimethylfuran 2(5H)lidene]malononitrile dye. *Spectrochim Acta, A: Mol Biomol Spectrosc* 75, 225–229. <https://doi.org/10.1016/j.saa.2009.10.015>
- 26 Megala, M. & Rajkumar, B.J. (2018). Molecular design of vinyl-functionalized quercetin dyes with different acceptors for dye-sensitized solar cells: theoretical investigation. *J Comput Electro* 17, 1153–1166. <https://doi.org/10.1007/s10825-018-1195-8>
- 27 Wang, H., Liu, Q., Liu, D., Su, R., Liu, J. & Li, Y. (2018). Computational Prediction of Electronic and Photovoltaic Properties of Anthracene-Based Organic Dyes for Dye-Sensitized Solar Cells. *Int J Photoenergy* 17, 4764830, <https://doi.org/10.1155/2018/4764830>
- 28 Pounraj, P., Mohankumar, V., Senthil Pandian, M. & Ramasamy, P. (2019). Donor substituted triphenylamine based sensitizers for dye sensitized solar cells (DSSC) application — DFT and TD-DFT approach. *AIP Conf Proc* 2115, 030345. <https://doi.org/10.1063/1.5113184>
- 29 Prabu, K.M., Agalya, P., Akila, K. & Suresh, S. (2019). Non-linear optical properties of carbazole based dyes modified with diverse spacer units for dye-sensitized solar cells: A first principle study. *AIP Conf Proc* 2177, 020072. <https://doi.org/10.1063/1.5135247>
- 30 Bonomo, M., Carella, A., Borbone, F., Rosato, L., Dini, D. & Gontrani, L. (2020). New pyran-based molecules as both n- and p-type sensitizers in semi-transparent Dye Sensitized Solar Cells, *Dyes and Pigments.* 175, 108140. <https://doi.org/10.1016/j.dyepig.2019.108140>
- 31 Lin, C., Liu, Y., Shao, D., Wang, W., Xu, H., Shao, C., Zhang, W. & Yang, Z. (2012). Density functional theory design of double donor dyes and electron transfer on dye/TiO<sub>2</sub>(101) composite systems for dye-sensitized solar cells. *RSC Adv* 11, 3071–3078. <https://doi.org/10.1039/D0RA08815C>
- 32 Pastore, M., Mosconi, E., de Angelis, F. & Gratzel, M. (2010). A computational investigation of organic dyes for dye-sensitized solar cells: Benchmark, strategies, and open issues. *J Phys Chem C* 114, 7205–7212. <https://doi.org/10.1021/jp100713r>

- 33 Estrella, L.L., Balanay, M.P. & Kim, D.H. (2016). The effect of donor group rigidification on the electronic and optical properties of arylamine-based metal-free dyes for dye-sensitized solar cells: a computational study. *J Phys Chem A*, 120, 5917-5927. <https://doi.org/10.1021/acs.jpca.6b03271>
- 34 Becke, A.D. (1993). Density functional thermo-chemistry. III. The role of exact exchange. *Journal of Physical Chemistry*, 98, 5648-5652. <https://doi.org/10.1063/1.464913>
- 35 Lee, C., Yang, W. & Parr, P.G. (1988). Development of the colle-salvetti correlation-energy formula into a functional of the electron density. *Phys Rev B* 37,785-789. <https://doi.org/10.1103/PhysRevB.37.785>
- 36 Spartan '14 wavefunction Inc. Irvine, USA (2014).
- 37 Delgado-Montiel, T., Baldenebro-López, J., Soto-Rojo, R. & Glossman-Mitnik D. (2020). Theoretical Study of the Effect of  $\pi$ -Bridge on Optical and Electronic Properties of Carbazole-Based Sensitizers for DSSCs. *Molecules* 25, 3670. <https://doi.org/10.3390/molecules25163670>
- 38 El-Shishtawy, R.M., Elroby, S.A., Asiri, A.M. & Müllen, K. (2016). Optical Absorption Spectra and Electronic Properties of Symmetric and Asymmetric Squaraine Dyes for Use in DSSC Solar Cells: DFT and TD-DFT Studies. *Int J Mol Sci* 17, 487. <https://doi.org/10.3390/ijms17040487>
- 39 Wazzan, N.A. (2019). A DFT/TDDFT investigation on the efficiency of novel dyes with ortho-fluorophenyl units (A1) and incorporating benzotriazole/benzothiadiazole/phthalimide units (A2) as organic photosensitizers with D-A2- $\pi$ -A1 configuration for solar cell applications. *J Comput Electron* 8, 375-395. <https://doi.org/10.1007/s10825-019-01308-4>
- 40 Lu, X., Wei, S., Wu, C.-M.L., Li, S. & Guo, W. (2011). Can Polypyridyl Cu(I)-based Complexes Provide Promising Sensitizers for Dye-Sensitized Solar Cells? A Theoretical Insight into Cu(I) versus Ru(II) Sensitizers. *J Phys Chem C* 115, 3753-3761. <https://doi.org/10.1021/jp111325y>
- 41 Soto-Rojo, R., Baldenebro-Lopez, J. & Glossman-Mitnik, D. (2015). Study of chemical reactivity in relation to experimental parameters of efficiency in coumarin derivatives for dye sensitized solar cells using DFT. *Phys Chem Chem Phys* 17, 14122-14129. <https://doi.org/10.1039/C5CP01387A>
- 42 Zhang, M-D, Xie, H-X, Ju, X-H, Qin, L., Yang, Q-X, Zheng, H-G & Zhou, X-F (2013). D-D- $\pi$ -A organic dyes containing 4,4'-di(2-thienyl)triphenylamine moiety for efficient dye-sensitized solar cells. *Phys Chem Chem Phys*, 15, 634-641. <https://doi.org/10.1039/C2CP42993D>
- 43 Parr, R.G., Szentpaly, L. & Liu, S. (1999). Electrophilicity Index. *Journal of American. Chemistry. Society* 121, 1922-1924. <https://doi.org/10.1021/cr040109f>
- 44 Afolabi, S.O., Semire, B., Akiode, O.K. & Idowu, M.A. (2022). Quantum study on the optoelectronic properties and chemical reactivity of phenoxazine-based organic photosensitizer for solar cell purposes. *Theo Chem Acc* 141, 22. <https://doi.org/10.1007/s00214-022-02882-w>
- 45 Koopmans, T. (1934). Ordering of Wave Functions and Eigenenergies to the Individual Electrons of an Atom. *Physica*, 1, 104-113. [https://doi.org/10.1016/S0031-8914\(34\)90011-2](https://doi.org/10.1016/S0031-8914(34)90011-2)
- 46 Afolabi, S.O., Semire, B., Akiode, O.K., Afolabi, T.A., Adebayo, G.A. & Idowu, M.A. (2020). Design and theoretical study of phenothiazine-based low bandgap dye derivatives as sensitizers in molecular photovoltaics. *Opt Quant Electronics* 52, 476. <https://doi.org/10.1007/s11082-020-02600-5>
- 47 Afolabi, S.O., Semire, B. & Idowu, M.A. (2021). Electronic and optical properties' tuning of phenoxazine-based D-A2- $\pi$ -A1 organic dyes for dye-sensitized solar cells. DFT/TDDFT investigations. *Heliyon*, 7, e06827. <https://doi.org/10.1016/j.heliyon.2021.e06827>
- 48 Semire, B., Oyebamiji, A.K. & Odunola, O.A. (2017). Tailoring of energy levels in (2Z)-2-cyano-2-[2-[(E)-2-[2-[(E)-2-(p-tolyl)vinyl]thieno[3,2-b]thiophen-5-yl]vinyl]pyran-4-ylidene]acetic acid derivatives via conjugate bridge and fluorination of acceptor units for effective D- $\pi$ -A dye-sensitized solar cells: DFT-TDDFT approach. *Res Chem Intermed* 43, 1863-1879. <https://doi.org/10.1007/s11164-016-2735-0>
- 49 Preat, J., Michaux, C., Jacquemin, D. & Perpete, E.A. (2009). Enhanced Efficiency of Organic Dye-Sensitized Solar Cells: Triphenylamine Derivatives. *J Phys Chem C* 113, 16821-16833. <https://doi.org/10.1021/jp904946a>
- 50 Rand, B.P., Genoe, J., Heremans, P., Poortmans, J. (2007). Solar cells utilizing small molecular weight organic semiconductors. *Progress in Photovoltaics: Res Appl* 15, 659-676. <https://doi.org/10.1002/pip.788>
- 51 Chou, C.T., Lin, C.H., Wu, M.H., Cheng, T.W., Lee, J.H., Liu, C.H., Tai, Y., Chattopadhyay, S., Wang, J.K., Chen, K.H., Chen, L.C. (2011). Tuning open-circuit voltage in organic solar cells by magnesium modified Alq(3). *J Appl Phys*, 110, 83104-831045. <https://doi.org/10.1063/1.3653259>
- 52 Zgou, H., Boussaidi, S., Eddiouane, A., Chaib, H., Tripathi, R.P., Ben, Hadda, T., Bouachrine, M. & Hamidi, M. (2016). New low band-gap conjugated organic materials based on fluorene, thiophene and phenylene for photovoltaic applications: Theoretical study. *Mater Today: Proc* 3(7), 2578-2586. <https://doi.org/10.1016/j.matpr.2016.04.005>
- 53 Ren, P., Sun, C., Shi, Y., Song, P., Yang, Y., Li, Y. (2019). Global performance evaluation of solar cells using two models: from charge-transfer and recombination mechanisms to photoelectric properties. *J Mater Chem C* 7, 1934-1947. <https://doi.org/10.1039/C8TC05660A>
- 54 Kacimi, R., Raftani, M., Abram, T., Azaid, A., Ziyat, H., Bejjit, L., Bennani, M.N., Bouachrine M. (2021). Theoretical design of D- $\pi$ -A system new dyes candidate for DSSC application. *Heliyon*. 7, e07171: <https://doi.org/10.1016/j.heliyon.2021.e07171>
- 55 Wang, H., Wang, B., Yu, J., Hu, Y., Xia, C., Zhang, J. & Liu, R. (2015). Significant enhancement of power conversion efficiency for dye sensitized solar cell using 1D/3D network nanostructures as photoanodes. *Scientific Reports* 5, 305. <https://doi.org/10.1038/srep09305>

- 56 Minaev, B.F., Baryshnikov, G.V. & Minaeva, V.A. (2012). Electronic structure and spectral properties of the triarylamine-dithienosilole dyes for efficient organic solar cells. *Dyes and Pigments*, 92(1), 531-536. <https://doi.org/10.1016/j.dyepig.2011.06.012>
- 57 Baryshnikov, G.V., Minaev, B.F., Myshenko, E.V. & Minaeva, V.A. (2013). Structure and electronic absorption spectra of isotruxene dyes for dye-sensitized solar cells: investigation by the DFT, TDDFT, and QTAIM methods. *Optics and spectroscopy*, 115, 484-490. <https://doi.org/10.1134/S0030400X13100020>
- 58 Oprea, C.I., Frecuş, B., Minaev, B.F. & Gîrţu, M.A. (2011). DFT study of electronic structure and optical properties of some Ru- and Rh-based complexes for dye-sensitized solar cells. *Molecular Physics*, 109 (21), 2511-2523. <https://doi.org/10.1080/00268976.2011.621454>
- 59 Minaev, B.F., Khomenko, E.M. & Yashchuk, L.B. (2009). Modeling the structure and spectral properties of sensitizing black dye for nanocrystalline TiO<sub>2</sub> solar cells. *Journal of Applied Spectroscopy*, 76 (6), 772-776. <https://doi.org/10.1007/s10812-010-9264-1>
- 60 Minaev, B., Li, X., Ning, Z., Tian, H. & Ågren, H. (2011). Organometallic materials for electroluminescent and photovoltaic devices. *Organic Light Emitting Diode—Material, Process and Devices, In Tech, Rieka*, 61-100. <https://doi.org/10.5772/21145>

#### Information about authors\*

**Obiyenwa, Gabriel Kehinde** — PhD, Assistant Professor, Department of Chemistry, Federal University, P.M.B 1154, Lokoja, Kogi State, Nigeria; e-mail: [gabriel.obiyenwa@fulokoja.edu.ng](mailto:gabriel.obiyenwa@fulokoja.edu.ng); <https://orcid.org/0000-0003-0184-8807>

**Semire, Banjo** (*corresponding author*) — PhD, Professor, Candidate of Computational Chemistry Laboratory, Department of Pure and Applied Chemistry, Ladoke Akintola University of Technology, PMB 4000, Ogbomoso, Nigeria; e-mail: [bsemire@lautech.edu.ng](mailto:bsemire@lautech.edu.ng); <https://orcid.org/0000-0002-4173-9165>

**Oyebamiji, Abel Kolawole** — PhD, Assistant Professor, Industrial Chemistry Programme, Bowen University, PMB 284, Iwo, Osun State, Nigeria; e-mail: [abel.oyebamiji@bowen.edu.ng](mailto:abel.oyebamiji@bowen.edu.ng); <https://orcid.org/0000-0002-8932-6327>

**Abdulsalami, Ibrahim Olasegun** — PhD, Senior Lecturer, Department of Chemistry, Nigerian Army University, PMB 1500, Biu, Bornu State, Nigeria; e-mail: [aiboldkip@gmail.com](mailto:aiboldkip@gmail.com); <https://orcid.org/0000-0001-5154-6407>

**Latona, Dayo Felix** — PhD, Associate Professor, Department of Pure and Applied Chemistry, Osun State University, 210001, Osogbo, Nigeria; e-mail: [dayo.latona@uniosun.edu.ng](mailto:dayo.latona@uniosun.edu.ng); <https://orcid.org/0000-0002-2722-6734>

**Adeoye, Moriam Dasola** — PhD, Professor, Department of Chemistry, Fountain University, Osogbo, P.M.B. 4491, Osun State, Nigeria; e-mail: [dasoladeoye@yahoo.com](mailto:dasoladeoye@yahoo.com); <https://orcid.org/0000-0002-1274-9452>

**Odunola, Olusegun Ayobami** — PhD, Professor, Department of Chemistry, Faculty of Natural and Applied sciences, Hallmark University, 122101, Ijebu-Itele, Ogun state, Nigeria; e-mail: [oaodunola@lautech.edu.ng](mailto:oaodunola@lautech.edu.ng); <https://orcid.org/0000-0001-6385-1257>

\*The author's name is presented in the order: *Last Name, First and Middle Names*